IEEE Access
Multidisciplinary ⋮ Rapid Review ⋮ Open Access Journal

Received March 9, 2021, accepted March 26, 2021, date of publication March 31, 2021, date of current version April 9, 2021.

Digital Object Identifier 10.1109/ACCESS.2021.3069985

Design of FIR Half-Band Filter With Controllable Transition-Band Steepness

WOON CHO, DAEWON CHUNG, YUNSUN KIM, INGYUN KIM, AND JOONHYEON JEON
Department of Electronics and Electrical Engineering, Dongguk University, Seoul 04620, South Korea

Corresponding author: Joonhyeon Jeon (memory@dgu.edu)

This work was supported in part by the Korea Institute of Energy Technology Evaluation and Planning under Grant 20194030202320, and in part by the Korea Evaluation Institute of Industrial Technology funded by the Ministry of Trade, Industry and Energy of the Republic of Korea under Grant 20012884.

ABSTRACT Maximally flat (MAXFLAT) half-band filters usually have wider transition-band than other filters although the frequency response is maximally flat (i.e., no ripples) in the passband and stopband. This is due to fact that the maximum possible number of zeros at z $= \pm 1$ is imposed in half-band close form solution, which leaves no degree of freedom, and thus no independent parameters for direct control of the frequency response. This paper describes a novel method for the design of FIR half-band filters with an explicit control of the transition bandwidth. The proposed method is based on a generalized Lagrange half-band polynomial (g-LHBP) with coefficients parameterizing a *0*-th coefficient h_0 and allows the frequency response of this filter type to be controllable by adjusting h_0. Then, h_0 is modeled as a steepness parameter of the transition-band and this is accomplished through theoretically analyzing a polynomial recurrence relation of the g-LHBP. This method also provides explicit formulas for direct computation of design parameters related to choosing a desired filter characteristic (by a reasonable trade-off between the transition-band sharpness and passband & stopband flatness). The examples are shown to provide a complete and accurate solution for the design of such filters with relatively sharper transition-band steepness than other existing half-band filters.

INDEX TERMS Maximally flat FIR filters, FIR digital filters, interpolator, closed-form polynomial, transition-band steepness.

I. INTRODUCTION

Maximally flat (MAXFLAT) filters are one of the most important types of non-recursive finite impulse response (FIR) filters and are applied when high stopband attenuation or smooth frequency response is desired [1]–[5]. The basic idea for the design of MAXFLAT FIR filters is to use a mathematically proved closed-form solution which satisfies MAXFLAT constraints at the ends of the frequency band and is mapped to the transfer function for the computation of coefficients of filters [6]–[13]. However, classical design involves approximation of the desired frequency response by some suitable closed-form polynomial [14]–[18] because such a closed-form solution mainly focuses on the flatness of the filter but not on the exact frequency response [11]–[13]. Several methods and implementation tricks have been proposed for the design of MAXFLAT FIR half-band filters [15], [16], [19], [20]. These filters have exact cutoff frequency at the middle of the frequency band $\omega = \pi / 2$ and allow computationally efficient implementations because almost half of their impulse response (IR) coefficients are zeros. However, their transition-band is relatively wider than other filters and can be narrowed only by increasing the length of the filter. Most of the popular MAXFLAT FIR half-band filters are designed by the Lagrange half-band polynomial (LHBP) which has the maximum number of zeros at $z = -1$ [21], [22]. This class of filters has many applications such as filter banks, wavelets-based compression, and multirate techniques [15], [16], [19], [23], [24]. However, similarly to the existing MAXFLAT FIR half-band filters, the LHBP filters do not also have any independent (''free'') parameters. In other words, there is no direct control over the frequency response of LHBP filters in order to achieve a reasonable trade-off between stopband attenuation and the width of the transition-band. This is due to fact that the maximum possible number of zeros

The associate editor coordinating the review of this manuscript and approving it for publication was Prakasam Periasamy.

at $z = -1$ is imposed on a half-band closed form solution, which leaves no degree of freedom, and thus no independent parameters.

To address such a narrow transition band issue in designing FIR filters so far, there have been a lot of efforts in the direction of frequency response control by utilizing various design technologies [14]–[19], [25]–[29]. Rodrigues and Pai introduced a sharp transition FIR filter design using sinusoidal functions of frequency to evaluate the impulse response coefficients in closed form [25]. This method allows closed-form parameters for simple and direct computation, but there occur non-negligible amplitude distortions in the stopband and passband. San-José-Revuelta *et al.* have reported an intelligence metaheuristic-based iterative method using multi-fitness function combined with a weighted error function [18]. However, this filter design has the disadvantage of requiring complicated and enormous computation processing for adjusting the ripples of the bands and the width of the transition-band. In contrast to previous studies [18], [25], Frequency Response Masking (FRM)-based filters outperform other designed filters in terms of the transition bandwidth and maximum passband ripple for a given order of filter within an acceptable limit [17], [19], [28]. Recently, Roy and Chandra reported enhanced FRM method using an interpolated band-pass filter, resulting in novel FRM-based filters with more excellent frequency characteristics [28]. However, this filter bank structure-based design requires high design complexity to obtain an interpolated prototype filter and two masking filters which configure the FRM filter bank. Moreover, there occur serious problems such as high group delay and the generation of aliasing band, and the magnitude response of this filter type never passes through the half-band cutoff frequency $\omega = \pi / 2$. Design methods mentioned above focus on realizing narrow transition band filters, but not half-band filters with narrow transition bandwidth. FIR half-band filter design should allow frequency control factors for narrow transition-band by considering limited frequency characteristics such that half of their coefficients are zero as well as being symmetrical. Khan and Ohba [30], Khan [31] reported FIR half-band filters with narrow transition-band that have their points of flatness at the middle point between the passband and stopband, but such a filter does not have any independent parameters to control the frequency response and the sharpness of the transition-band can be achieved with a comparatively higher value of filter length. Ma *et al.* have proposed a cascaded half-band filter design by controlling stopband attenuation for a fixed transition bandwidth [16]. This multistage algorithm allows computation reduction of more than 4% per input sample as compared to conventional filters, but there exists the limitation of half-band filter design because a heuristic threshold value is required to meet a specified narrow transition band. Hence, the half-band design is needed for highly accurate filters with controllable frequency characteristics – i.e., with a reasonable trade-off between the transition-band sharpness and passband & stopband ripples.

In this paper, our aim is to design FIR half-band filters with controllable frequency responses. This is achieved by starting with a closed-form half-band polynomial. Design regularity is to impose zeros at $z = -1$ on the half-band polynomial, and then, the number of zeros must be less than the maximum possible. First, we present a generalized Lagrange half-band polynomial (g-LHBP) whose all IR coefficients are represented with a *0*-th IR coefficient h_0 for a given order of filter. Then, through analyzing a linear recursive relation of the g-LHBP, h_0 is parameterized to directly control the transition-band steepness (or width) of this filter type. Using the new approach, we develop a design procedure that is computationally more efficient and accurate than the previous methods. Also, this new technique provides explicit formulas for the performance evaluation of a resulting filter and consequently, allows unusual flexibility in choosing a best filter with a desired magnitude response characteristic (namely, with trade-off between the transition-band sharpness and passband & stopband flatness). Design of FIR half-band filters through this new approach gives an additional insight into the physical significance of some independent parameters for an explicit control of the frequency response.

This paper is organized as follows. In Section II we derive a generalized Lagrange half-band polynomial with h_0. In Section III, an objective control function is derived from a recursive relation of the g-LHBP and analyzed to parameterize h_0 as a steepness control factor of the transition-band. Additionally, various formulas are proposed to design this filter type efficiently and accurately with a narrow transition band. In Section IV, design examples that demonstrate the power of the new technique are shown. In addition, to show the effectiveness of the proposed method, g-LHBP filters are compared to existing state-of-art filters. Conclusions are drawn in Section V.

II. GENERALIZED LAGRANGE HALF-BAND POLYNOMIAL

When Let $H(z)$ be a general symmetric FIR half-band filter of type II (odd number of odd-symmetric coefficients) with the real impulse response h_n of order $4K - 2$, which can be written as

$$H(z) = z^{-(2K-1)} Q_K(z) \tag{1}$$

by using the transfer function

$$Q_K(z) = 0.5 + \sum_{n=1}^{K} h_{2K-2n}(z^{-(2n-1)} + z^{2n-1}) \tag{2}$$

where $Q_K(z)$ represents a zero-phase half-band lowpass filter. Design of MAXFLAT FIR half-band filters for the filter type of (2) can be easily realized by using some suitable closed-form polynomial [10]–[13], [22] which is then mapped to the filter function by certain transformations. Regularity is imposed in the design of $Q_K(z)$ by focusing $Q_K(z)$ to have zeros at $z = -1$, i.e., terms of the form $(1+z^{-1})$. One of most popular methods for designing MAXFLAT FIR half-band filters of order $4K - 2$ is to use a Lagrange half-band polynomial (LHBP) [21], [22] as below

$$Q_K(z)_{LHBP} = z^K \left(\frac{1+z^{-1}}{2}\right)^{2K} \times \left\{\sum_{\ell=0}^{K-1} d_{K,\ell}\left(\frac{2-z-z^{-1}}{4}\right)^{\ell}\right\} \quad (3)$$

where $d_{K,\ell}$ is

$$d_{K,\ell} = \binom{K+\ell-1}{\ell} = \frac{(K+\ell-1)!}{(K-1)! \times \ell!} \quad (4)$$

The LHBP has a maximum number of zeros at $z = -1$, and thus, it has a maximally flat response at $\omega = \pi$, i.e.,

$$\left.\frac{\partial^k Q_K(\omega)_{LHBP}}{\partial \omega^k}\right|_{\omega=\pi} = 0, \quad k = 0, 1, 2, \ldots, 2K-1 \quad (5)$$

It is shown that the LHBP filter does not have any independent ("free") parameters as described in (3) and there is no direct control over the frequency response of the filter obtained by the LHBP.

Let us define that $Q_K(z)$ shown in (2) has $2(K-1)$ zeros at $z = -1$: i.e.,

$$\left.\frac{\partial^k Q_K(\omega)}{\partial \omega^k}\right|_{\omega=\pi} = 0, k = 0, 1, 2, \ldots, 2K-3 \quad (6)$$

The condition of (6) are imposed on (2), and using Lagrange interpolation at coincident points [30], [31] so that $Q_K(z)$ has a recursive relationship similar to (3), a closed-form half-band polynomial, called a generalized LHBP (g-LHBP), can be obtained in terms of h_0 as (see (A.12) in Appendix A)

$$Q_K(z) = z^{K-1}\left(\frac{1+z^{-1}}{2}\right)^{2(K-1)} \left\{\sum_{\ell=0}^{K-2} d_{K-1,\ell} \times \left(\frac{2-z-z^{-1}}{4}\right)^{\ell} + (-1)^{K-1}2^{4K-2}h_0 \times \left[\frac{1}{2}\left(\frac{2-z-z^{-1}}{4}\right)^{K-1} \left(\frac{2-z-z^{-1}}{4}\right)^{K}\right]\right\} \quad (7)$$

It is seen that (7) is identical to LHBP of (3) if h_0 is given as

$$h_0 = (-1)^{K-1}\frac{d_{K,K-1}}{2^{4K-2}} \quad (8)$$

where (8) is obtained by additionally imposing a zero at $z = -1$ on (7). For a general closed-form expression, mapping (7) to

$$Q_K(z) = z^{K-1}\left(\frac{1+z^{-1}}{2}\right)^{2(K-1)} \left\{g_K + \sum_{\ell=1}^{K} g_{K-\ell}\left(z^{\ell} + z^{-\ell}\right)\right\} \quad (9)$$

we can obtain the interpolation coefficients $g'_{\ell}s(\ell = 0, 1, 2, \ldots, K)$ in terms of h_0 and K as (see (A.13) in Appendix A)

$$g_{\ell} = (-1)^{K-\ell}\sum_{j=2}^{\ell}\frac{d_{K-1,K-j}}{2^{2(K-j)}}\binom{2(K-j)}{l-j} + (-1)^{\ell+1}2^{2K-1}h_0\left\{\binom{2(K-1)}{\ell-1} - \frac{1}{2}\binom{2K}{l}\right\} \quad (10)$$

Computation of IR coefficients h_n's, using (10), was reported in [13], [24]. In a similar way, mapping (9) into (2), we can get

$$h_n = \frac{1}{2^{2(K-1)}}\left\{\sum_{\ell=0}^{K}\binom{2(K-1)}{n-\ell}g_{\ell} + \sum_{\ell=1}^{K}\binom{2(K-1)}{n-\ell-K}g_{K-\ell}\right\}, \quad n = 1, 2, 3, \ldots, 2K-2 \quad (11a)$$

or equivalently,

$$h_{2n-1} = 0 \text{ and } h_{2n} = \frac{1}{2^{2(K-1)}}\left\{\sum_{\ell=0}^{K}\binom{2(K-1)}{2n-\ell}g_{\ell} + \sum_{\ell=1}^{K}\binom{2(K-1)}{2n-\ell-K}g_{K-\ell}\right\}, \quad n = 1, 2, 3, \ldots, K-1 \quad (11b)$$

where $\binom{A}{B} = 0$, if $A < B$ or $B < 0$.

Note that when substituting (10) into (11a), the odd number indexed coefficients are 0, as shown in (11b) – i.e., h_{2n-1}'s = 0. From (7) the frequency response of this class of filters can be also expressed in terms of K and h_0 as

$$Q_K(\omega) = \left(cos\frac{\omega}{2}\right)^{2(K-1)}\left\{\sum_{\ell=0}^{K-2} d_{K-1,\ell} \times \left(sin\frac{\omega}{2}\right)^{2\ell} + (-1)^{K-1}2^{4K-2}h_0 \times \left[\frac{1}{2}\left(sin\frac{\omega}{2}\right)^{2(K-1)} - \left(sin\frac{\omega}{2}\right)^{2K}\right]\right\} \quad (12)$$

It is shown from (12) that the frequency response is ever controllable by introducing h_0 as a parameter and thus, various g-LHBP filters with trade-off between transition bandwidth and magnitude flatness can be obtained. In addition, (11), using (10), also allows direct computation of the coefficients if h_0 is chosen. However, for a given order of filter $4K-2$, there are an infinite number of FIR half-band filters due to the large dynamic range of h_0. Thus, h_0 must be modeled as a controllably independent parameter which can be optimized and determined to obtain such a filter with the desired magnitude characteristic. This will be explained in the next section.

III. OBJECTIVE CONTROL FUNCTION OF G-LHBP: TRANSITION-BAND STEEPNESS PARAMETER h_0

Now, through the analysis of (12), we consider how to derive h_0 as a steepness parameter for the direct control of the transition-band edges. Design regularity is here to determine h_0 so that g-LHBP filters have tolerant magnitude distortion (ripples) but narrow transition band.

From the recursive relation of $Q_K(z)$ (see (A.2) in Appendix A) it is shown that $A_K(z)$ plays a role as an objective function for the extension of $Q_{K-1}(z)_{LHBP}$ to $Q_K(z)$ (where $Q_{K-1}(z)_{LHBP}$ and $A_K(z)$ are also indicated in (A.3) and (A.12) of Appendix A, respectively). Remarkably, $Q_K(\omega)$ described in (12) can be also rewritten as a recursive relation

$$Q_K(\omega) = Q_{K-1}(\omega)_{LHBP} + A_K(\omega) \tag{13}$$

where $Q_{K-1}(z)_{LHBP}$ and $A_K(\omega)$ are given, respectively, as

$$Q_{K-1}(\omega)_{LHBP} = \left(cos\frac{\omega}{2}\right)^{2(K-1)} \sum_{\ell=0}^{K-2} d_{K-1,\ell} \left(sin\frac{\omega}{2}\right)^{2\ell} \tag{14}$$

$$A_K(\omega) = (-1)^{K-1} 2^{2(K-1)} h_0 \,(cos\omega)\,(sin\omega)^{2(K-1)} \tag{15}$$

(Here $A_K(\omega)$ has been simplified with $sin\omega = 2sin\frac{\omega}{2}cos\frac{\omega}{2}$). Hence, we can be sure from (13) that for a given K, since $Q_{K-1}(\omega)_{LHBP}$ is a known MAXFLAT lowpass function, $A_K(z)$ characterizes $Q_K(\omega)$ in terms of h_0. In other words, we can describe the effect of h_0 on $Q_K(\omega)$ through the analysis of $A_K(\omega)$. From (15) $A_K(\omega)$ passing through zero value at $\omega = 0$, $\omega = \pi / 2$, and $\omega = \pi$ exhibits a "anti-symmetric sinusoid-like shape" with respect to $\pi / 2$ as the center point in the range of $0 \leq \omega \leq \pi$. Thus, there are two anti-symmetric peak values that are available to assist in identifying influential observations of $A_K(\omega)$ in terms of h_0 on $Q_K(\omega)$. If ω_p^+ and ω_p^- are the two peak frequencies of $A_K(\omega)$, we can obtain in terms of K, by solving $\partial A_K(\omega) / \partial\omega = 0$ at $\omega = \omega_p^{\pm}$, as

$$\omega_p^{\pm} = arccos\left(\pm\frac{1}{\sqrt{2K-1}}\right), 0 < \omega_p^+ < \pi/2 < \omega_p^- < \pi \tag{16}$$

and then, the two peak values $A_K(\omega_p^+)$ and $A_K(\omega_p^-)$ are obtained, by substituting (16) into (15), as

$$A_K(\omega_p^{\pm}) = \pm(-1)^{K-1}2^{2K-1}h_0 \times \frac{1}{\sqrt{2K-1}}\left(1-\frac{1}{(2K-1)}\right)^{K-1} \tag{17}$$

where $\omega_p^{\pm}$ (double signs in same order) denotes ω_p^+ and ω_p^-, and is related to $\omega_p^+ + \omega_p^- = \pi$ from $\cos(\omega_p^+ + \omega_p^-) = -1$. Especially, since both $Q_{K-1}(z)_{LHBP}$ and $A_K(\omega)$ is anti-symmetric with respect to $\omega = \pi / 2$ as the center point in $0 \leq \omega \leq \pi$, $Q_{K-1}(\omega_p^{\pm})_{LHBP}$ and $A_K(\omega_p^{\pm})$ satisfy the following properties:

$$Q_{K-1}(\omega_p^+)_{LHBP} + Q_{K-1}(\omega_p^-)_{LHBP} = 1 \tag{18a}$$

$$A_K(\omega_p^+) + A_K(\omega_p^-) = 0 \tag{18b}$$

From the relationship of (13), these anti-symmetric properties at $\omega = \omega_p^+$ and ω_p^- result in

$$Q_K(\omega_p^+) + Q_K(\omega_p^-) = 1 \tag{19}$$

Substituting (17) into (13) with $\omega = \omega_p^{\pm}$ and simplifying with respect to h_0, we can obtain

$$h_0 = \frac{Q_K(\omega_p^{\pm}) - Q_{K-1}(\omega_p^{\pm})_{LHBP}}{(-1)^{K-1}2^{2K-1}\left(\frac{1}{\sqrt{2K-1}}\right)\left(1-\frac{1}{(2K-1)}\right)^{K-1}} \tag{20}$$

where two h_0's (double signs in same order) have an equivalent value since $Q_K(\omega_p^+) - Q_{K-1}(\omega_p^+)_{LHBP} = -Q_K(\omega_p^-) + Q_{K-1}(\omega_p^-)_{LHBP}$ from the properties of (18a) and (19). It is indicated that using (20) to get h_0 in (12) yields $Q_K(\omega)$ that exactly passes through $Q_K(\omega_p^+)$ and $Q_K(\omega_p^-)$ at $\omega = \omega_p^+$ and ω_p^-. Thus, using ω_p^+ and ω_p^- as two transition-band edge frequencies of this filter (i.e., upper and lower edge frequencies), we can define a transition-band slope of this class of g-LHBP filters as below

$$slope_K = \frac{Q_K(\omega_p^-) - Q_K(\omega_p^+)}{\omega_p^- - \omega_p^+} \tag{21}$$

It is seen, based on (21), that h_0 shown in (20) can be used as a steepness parameter to directly control the transition-band slop represented with $Q_K(\omega_p^+)$ and $Q_K(\omega_p^-)$ for a given K. Consequently, substituting the upper edge $Q_K(\omega_p^+) = \gamma$ (then, the lower edge becomes $Q_K(\omega_p^-) = 1 - \gamma$ from (19)) into respectively (20) and (21), we can rewrite h_0 and $slope_K$ in terms of γ as

$$h_{0,\gamma} = \frac{\gamma - Q_{K-1}(\omega_p^+)_{LHBP}}{(-1)^{K-1}2^{2K-1}\left(\frac{1}{\sqrt{2K-1}}\right)\left(1-\frac{1}{(2K-1)}\right)^{K-1}} \tag{22}$$

$$slope_{K,\gamma} = \frac{1-2\gamma}{arccos\left(1-\frac{2}{2K-1}\right)} \tag{23}$$

where $\omega_p^- - \omega_p^+$ has been obtained by using (16) on product-to-sum transformation $(\cos\omega_p^-)\,(\cos\omega_p^+) = 1/2\ \{\cos(\omega_p^- - \omega_p^+)\ \cos(\omega_p^- + \omega_p^+)\}$. Then, it can be seen from (23) that the steepness of the transition-band is controllable by changing the upper-edge parameter γ for a given K. To determine $h_{0,\gamma}$ according to (22), so that a g-LHBP filter has a relatively narrower transition band than a MAXFLAT g-LHBP filter, γ has to be chosen within the limits of $Q_K(\omega_p^+)_{MAXFLAT} < \gamma \leq 1$

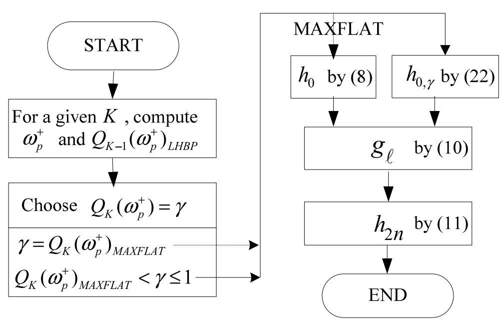

FIGURE 1. Design procedure to obtain g-LHBP filters with narrow transition band.

where $Q_K(\omega_p^+)_{MAXFLAT}$ can be obtained according to (8), (12), and (16) (respectively, h_0, $Q_K(\omega)_{MAXFLAT}$, and ω_p^+). Then, note that for a given K, $h_{0,\gamma}$ computed by substituting $\gamma = Q_K(\omega_p^+)_{MAXFLAT}$ into (22) is equal to that h_0 by (8), and $Q_K(\omega)$ using h_0 with $\gamma > 1$ has sharper transition-band but larger distortion response in the passband and the stopband.Based on the results so far, Fig. 1 shows a design procedure to permit direct and simple computation of coefficients of g-LHBP filters.

Performance evaluation: Choosing $h_{0,\gamma}$ with γ within $Q_K(\omega_p^+)_{MAXFLAT} < \gamma \leq 1.0$ may cause overshoot and undershoot in the passband and the stopband, respectively. Hence, it is necessary to verify whether such distortions are tolerant or not. To calculate the passband and stopband peak errors due to using (22), let ω_d^+ and ω_d^- be the peak overshoot and undershoot frequencies. Then, $Q_K(\omega_d^+)$ and $Q_K(\omega_d^-)$ become peak values in the passband and the stopband, respectively. Solving $\partial Q_K(\omega) \,/\, \partial\omega = 0$ at $\omega = \omega_d^\pm$, $\omega_d^\pm$ can be obtained in terms of K and $h_{0,\gamma}$ as

$$\omega_d^\pm = arccos \left(\pm\sqrt{\frac{1}{2K-1}\left\{1+(-1)^{K-1}\frac{(2K-3)}{2^{4(K-1)}h_{0,\gamma}}\binom{2(K-2)}{K-2}\right\}}\right) \tag{24}$$

where $\omega_d^\pm$(double signs in same order) denotes ω_d^+ and ω_d^-, satisfying such that $\omega_d^+ + \omega_d^- = \pi$ from $\cos(\omega_d^+ + \omega_d^-) = -1$. In the similar way of deriving (19), $Q_{K-1}(\omega_d^\pm)_{LHBP}$ and $A_K(\omega_d^\pm)$ have the following properties, respectively

$$Q_{K-1}(\omega_d^+)_{LHBP} + Q_{K-1}(\omega_d^-)_{LHBP} = 1 \; and$$
$$A_K(\omega_d^+) + A_K(\omega_d^-) = 0 \tag{25}$$

to yield

$$Q_K(\omega_d^+) + Q_K(\omega_d^-) = 1 \tag{26}$$

From (26) it can be seen that the maximum overshoot ripple $\delta_{K,\gamma}^{max}$ due to $Q_K(\omega_d^+)$ is equal to the magnitude of the peak undershoot $Q_K(\omega_d^-)$ as follows:

$$\delta_{K,\gamma}^{max} = Q_K(\omega_d^+) - 1 = -Q_K(\omega_d^-) \tag{27}$$

where $\delta_{K,\gamma}^{max}$ is zero (i.e., $\delta_{K,\gamma}^{max} = 0$) if $h_{0,\gamma}$ is chosen according to (8) for the design of g-LHBP filters with MAXFLAT response. From (16) and (24) the inequality relation between $\omega_p^\pm$ and $\omega_d^\pm$ is $0 < \omega_d^+ < \omega_p^+ < \pi/2 < \omega_p^- < \omega_d^- < \pi$ and this results in $Q_K(\omega_d^+) > Q_K(\omega_p^+) > Q_K(\omega_p^-) > Q_K(\omega_d^-)$ due to $A_K(\omega_p^+) > A_K(\omega_d^+) > A_K(\omega_d^-) > A_K\omega_p^-)$. Fig. 2, in the case of $K = 3$, shows these parameters on the frequency responses of two g-LHBP filters where two h_0's have been chosen according to (22) with $\gamma = 1.0$ and (8) (equal to (22) with $\gamma_{MAXFLAT} = 0.8667$), respectively. It is shown that using (22) allows g-LHBP filters with narrow transition band but distortion such as overshoot and undershoot in the passband and the stopband, Hence, there still remains whether or not this undesired distortion due to the use of $h_{0,\gamma}$ is within the limit acceptable to the design of such filters with tolerant magnitude distortion but narrow transition band. Such performance evaluations are verified through design examples discussed in the next section.

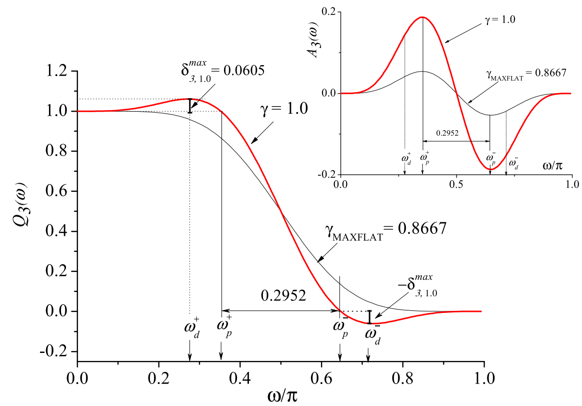

FIGURE 2. The frequency responses of two g-LHBP filters for a given $K = 3$; MAXFLAT filter (black solid line) and narrow transition band filter (red-bold line).

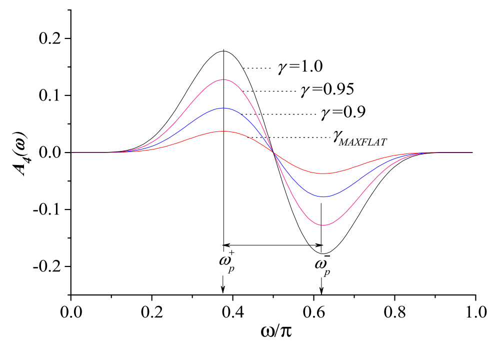

FIGURE 3. The frequency responses due to γ for a given $K = 4$: $A_4(\omega)$.

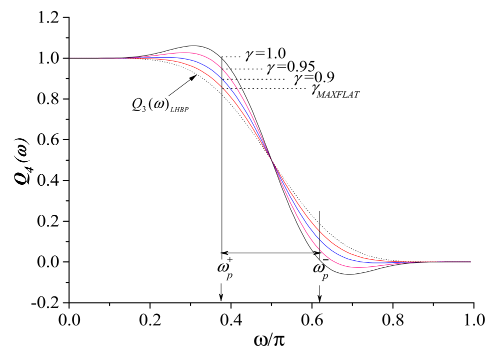

FIGURE 4. The frequency responses due to γ for a given $K = 4$: $Q_4(\omega)$.

IV. DESIGN EXAMPLES

In this section, through the design examples of g-LHBP lowpass filters, we demonstrate the usefulness of the proposed method, and verify that that the performance parameters derived above are accurate.

TABLE 1. Related parameters of Fig. 3 and Fig. 4.

Parameters	Characteristics of four g-LHBP filters due to various $\gamma = Q_4(\omega_p^+)$				Related Equation
	$\gamma_{MAXFALT} = 0.8592$	$\gamma = 0.9$	$\gamma = 0.95$	$\gamma = 1.0$	
order of filter	$14(K = 4)$				$4K - 2$
ω_p^+/π	0.3766				(16)
ω_p^-/π	0.6234				
$Q_3(\omega_p^+)_{LHBP}$	0.8220				(31)
$Q_3(\omega_p^-)_{LHBP}$	0.1780				
$h_{0,\gamma}$	-0.00122070	-0.00255885	-0.004201355	-0.00584116	(8) and (33)
$A_4(\omega_p^+)$	0.0372	0.0780	0.1280	0.1780	(32)
$A_4(\omega_p^-)$	-0.0372	-0.0780	-0.1280	-0.1780	
$Q_4(\omega_p^+)$	0.8592	0.9000	0.9500	1	(31) + (32) by (13)
$Q_4(\omega_p^-)$	0.1408	0.1000	0.0500	0	
ω_d^+/π	0	0.2335	0.2847	0.3079π	(24)
ω_d^-/π	1	0.7665	0.7153	0.6921π	
$Q_3(\omega_d^+)_{LHBP}$	1	0.9826	0.9516	0.9288	(31)
$Q_3(\omega_d^-)_{LHBP}$	0	0.0174	0.0484	0.0712	
$A_4(\omega_d^+)$	0	0.0219	0.0757	0.1322	(32)
$A_4(\omega_d^-)$	0	-0.0219	-0.0757	-0.1322	
$Q_4(\omega_d^+)$	1	1.0045	1.0273	1.0610	(31) + (32) by (13)
$Q_4(\omega_d^-)$	0	-0.0045	-0.0273	-0.0610	
$slope_{4,\gamma}$	-2.9117	-3.2421	-3.6474	-4.0527	(23)
$\delta_{4,\gamma}^{max}$	0	0.0045	0.0273	0.0610	(27)

For example, in the case of $K = 4$ (i.e., the order of filter is such that $4K - 2 = 14$), a general form for the g-LHBP of order 14 can be given from (9) as

$$Q_4(z) = z^3 \left(\frac{1+z^{-1}}{2}\right)^6 \left\{g_4 + \sum_{\ell=1}^{4} g_{4-\ell}(z^\ell + z^{-\ell})\right\} \quad (28)$$

Then, $g_\ell' s(\ell = 0, 1, 2, \ldots, 4)$ are obtained from (10) as

$$g_0 = 2^6 h_0,\ g_1 = -6 \cdot 2^6 h_0,\ g_2 = 3/8 + 16 \cdot 2^6 h_0,$$
$$g_3 = -9/4 - 26 \cdot 2^6 h_0,\ g_4 = 19/4 + 30 \cdot 2^6 h_0 \quad (29)$$

to yield the transfer function of the form shown in (2), which is expressed as

$$Q_4(z) = h_0 z^{-7} + \left(\frac{3}{2^9} - 5h_0\right) z^{-5} + \left(\frac{-25}{2^9} + 9h_0\right) z^{-3} + \left(\frac{75}{2^8} - 5h_0\right) z^{-1} + 0.5 \left(\frac{75}{2^8} - 5h_0\right) z + \left(\frac{-25}{2^9} + 9h_0\right) z^3 + \left(\frac{3}{2^9} - 5h_0\right) z^5 + h_{0,\gamma} z^7 \quad (30)$$

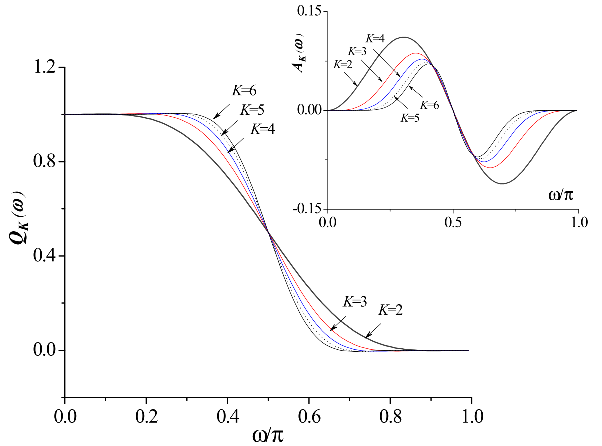

FIGURE 5. The frequency responses of g-LHBP filters due to K: $\gamma = 0.9$.

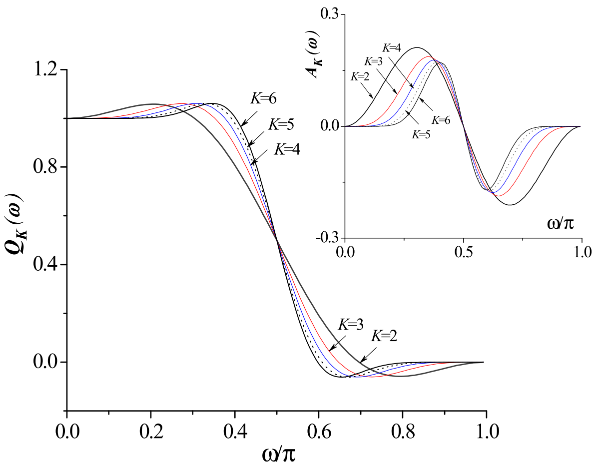

FIGURE 6. The frequency responses of g-LHBP filters due to K: $\gamma = 1.0$.

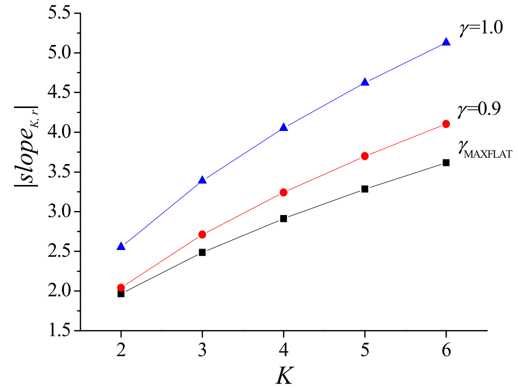

FIGURE 7. The performance comparison (from Table 3) for a given K and γ: $|slope_{K,\gamma}|$.

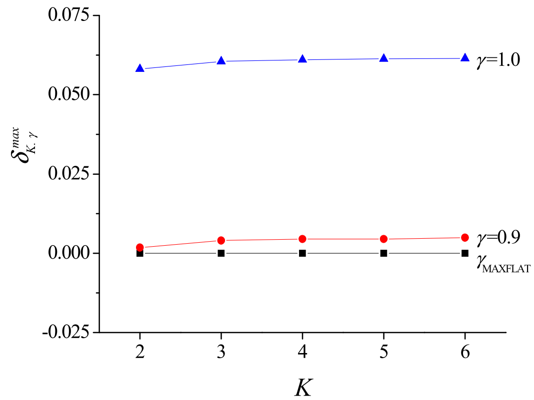

FIGURE 8. The performance comparison (from Table 3) for a given K and γ: $\delta_{K,\gamma}^{max}$.

where $h_{2n}(n = 1, 2, 3)$ is obtained by substituting (29) into (11b) with $K = 4$. Note that the odd number indexed coefficients of the half-band filter given by (2) are zero – i.e., $h_{2n-1}(n = 1, 2, 3)$. The frequency response of $Q_4(z)$ is such that from (13) $Q_4(\omega) = Q_3(\omega)_{LHBP} + A_4(\omega)$ where $Q_3(\omega)_{LHBP}$ and $A_4(\omega)$ are given, respectively from (14) and (15), as

$$Q_3(\omega)_{LHBP} = \left(cos\frac{\omega}{2}\right)^6 \left\{1 + 3\left(sin\frac{\omega}{2}\right)^2 + 6\left(sin\frac{\omega}{2}\right)^4\right\} \tag{31}$$

$$A_4(\omega) = -h_0 2^6 (cos\omega)(sin\omega)^6 \tag{32}$$

Then, h_0 are obtained, by substituting $K = 4$ into (22), as

$$h_{0,\gamma} = -\frac{\sqrt{7}^7}{2^{10} \cdot 3^3}\left\{\gamma - Q_3(\omega_p^+)_{LHBP}\right\} \tag{33}$$

where choosing $K = 4$ yields $\omega_p^+ = 0.3766\pi$ and $Q_3(\omega_p^+)_{LHBP} = 0.8220$ from (16) and (31), respectively. To show the effectiveness of the proposed method, the performance evaluation is carried out with four g-LHBP filters using four $h_{0,\gamma}$'s with $\gamma = MAXFLAT$, 0.9, 0.95, and 1.0 where $\gamma = MAXFLAT$ means the use of (8) for $h_{0,\gamma}$ – i.e., $h_{0,\gamma} = h_0 = -d_{4,3}/\ 2^{14}$ that is equal to substituting $\gamma_{MAXFLAT} = 0.8592$ into (33). Fig. 3 and Fig. 4 shows $A_4(\omega)$ and $Q_4(\omega)$ due to four $h_{0,\gamma}$'s and the related parameters are also indicated in Table 1. It is shown that the g-LHBP filters can have, by controlling $h_{0,\gamma}$ in (30), tolerant distortions but relatively narrow transition bands – i.e., $0 < \delta_{4,\gamma}^{max} \leq 0.0610$ in $0.8592 < \gamma \leq 1.0$ but $2.9117 < |Slope_{4,\gamma}| \leq 4.0527$. Especially, taking $\gamma = 0.9$ yields the g-LHBP filter that has an approximately flat magnitude response similar to the MAXFLAT FIR filter (substituting $\gamma_{MAXFLAT}$) but relatively narrower transition band.

Table 2 indicates g_ℓ's and h_n's of two filters using $h_{0,\gamma}$'s with $\gamma_{MAXFLAT}$ and $\gamma = 1.0$ where g_ℓ's and h_n's have been chosen according to (10) and (11), respectively.

For additional examples, Fig. 5 and Fig. 6 show g-LHBP filters with various K, and the related parameters of the filters are also indicated in Table 3. It can be found that as γ increases for a given K, the steepness of the transition-band slope increases rapidly but the amplitude distortion $(\delta_{K,\gamma}^{max})$ increases very slightly. The more K increases, the

TABLE 2. Coefficients of the two g-LHBP filters for $K = 4$.

	h_0 by (8) (: $\gamma_{MAXFALT} = 0.8592$)	$h_{0,1.0}$ by (37) with $\gamma = 1.0$
g_0	-0.078124998	-0.373834144
g_1	0.468749990	2.243004864
g_2	-0.874999974	-5.606346304
g_3	-0.218750042	7.469687744
g_4	2.406250048	-6.465024320
h_0	-0.001220703	-0.005841156
h_2	0.011962891	0.035065168
h_4	-0.059814453	-0.101398552
h_6	0.299072266	0.322174543
h_7	0.5	0.5

TABLE 3. Related parameters of Fig. 5 and Fig. 6 for $\gamma_{MAXFLAT}$, $\gamma = 0.9$, and $\gamma = 1.0$.

Parameters		K ($4K$ - 2) [a]			
		2(6)	3(10)	5(18)	6(22)
MAXFLAT by (8)	$h_{0,MAXFLAT}$	-0.03125000	0.00585938	-0.00026703	-0.00006008
	$slope_{K,MAXFLAT}$	-1.9646	-2.4848	-3.2832	-3.6166
	$\delta^{max}_{K,MAXFLAT}$	0.0000	0.0000	0.0000	0.0000
$\gamma = 0.9$	$h_{0,0.9}$	-0.03615381	0.00949352	-0.00068793	-0.00018373
	$slope_{K,0.9}$	-2.0417	-2.7103	-3.6978	-4.1029
	$\delta^{max}_{K,0.9}$	0.0018	0.0040	0.0048	0.0049
$\gamma = 1.0$	$h_{0,1.0}$	-0.06862976	0.02041182	0.00162649	-0.00044455
	$slope_{K,1.0}$	-2.5521	-3.3879	-4.6222	-5.1287
	$\delta^{max}_{K,1.0}$	0.0581	0.0605	0.0613	0.0614

[a]The ($4K$ - 2) denotes the order of filter and the related parameters of the filters, in the case of K = 4, have been indicated in Table I.

greater effect it can have, as shown in Fig. 7 and Fig. 8 that demonstrates the performance of g-LHBP filters for a given K and γ. In addition, Table 4 shows the comparison of the proposed method with the previous state-of-the-art works, where examples given in [16]–[19], [25], [28] have been considered for comparison purposes. It can be seen that the g-LHBP filters outperform the other designed filters in terms of transition bandwidth and peak-to-peak passband/stopband ripples. Particularly, it also appears the FRM-based filter suggested by Roy and Chandra [28] has relatively narrow transition bandwidth as compared to the g-LHBP filter, but non-negligible ripples take place in the stopband apart from complicated problems due to FRM bank structure-based filter form. Consequently, these examples demonstrate that the proposed method derives flexible FIR half-band filters with controllable frequency characteristics – i.e., with a reasonable trade-off between the transition-band sharpness and passband & stopband ripples.

TABLE 4. Comparison of proposed *g*-LHBP filter and previous narrow transition-band filters.

Design Method	Filter Order (N)	Transition-bandwidth (rad/ π)	Peak-to-peak ripple in the passband	Peak-to-peak ripple in the stopband
Ref.[18]	70	0.077	0.17234	6.4 x10^{-6}
g-LHBP	70	0.051	3.81x10^{-5}	
Ref.[16]	86	0.081	0.00138	0.00231
g-LHBP	86	0.044	4.07x10^{-5}	
Ref.[17]	100	0.024	0.00277	0.15882
g-LHBP	98	0.039	4.28x10^{-5}	
Ref.[28]	100	0.015	0.00104	0.01413
g-LHBP	102	0.017	0.00039	
Ref.[25]	270	0.15	0.03442	0.02377
g-LHBP	270	0.022	4.91x10^{-5}	
Ref.[19]	306	0.034	0.00024	0.00028
g-LHBP	306	0.015	5.14x10^{-5}	

※A peak-peak ripple (overshoot) value in the passband of a g-LHBP filter is equal to that (undershoot) in the stopband, as shown in figures and Table III. In addition, γ of *g*-LHBP filters is calculated by applying the transition bandwidth and filter order of the corresponding compared filter into (23), and it is determined within the limit of $\gamma_{MAXFALT} < \gamma < 1$.

V. CONCLUSION

The Problems with wide transition-band always arise in MAXFLAT FIR half-band filter design which leaves no degree of freedom (i.e., independent parameters) to control the frequency response by some closed-form polynomial.

In this paper, we have proposed a new method to design FIR half-band filters with an explicit control of the transition-band steepness. For this purpose, we have developed a generalized Lagrange half-band polynomial parameterizing *0*-th coefficient h_0 and have provided a solution to use h_0 as a transition-band steepness parameter of this filter type. In addition, new formulas have been given for direct and simple computation of parameters in closed form. The examples were also shown to verify the performance of this class of filters with tolerant ripple but relatively narrower transition band. Hence, a solution to the problem encountered in the previous methods is found.

APPENDIX A
DERIVATION OF THE G-LHBP

From (2) the transfer function of order $4K-2(=2N)$ can be rewritten by

$$\begin{aligned} Q_K(z) = & h_0 z^{-(2K-1)} + h_2 z^{-(2K-3)} + \ldots + h_{2K-4} z^{-3} \\ & + h_{2K-2} z^{-1} + 0.5 + h_{2K-2} z + + h_{2K-4} z^3 \\ & + \ldots + h_2 z^{2K-3} + h_0 z^{2K-1} \end{aligned} \tag{A.1}$$

The flatness condition of (6) is imposed on (A.1)-i.e., $2(K-1)$ zeros at $z=-1$, and using Lagrange interpolation at coincident points [24], [30], $Q_K(z)$ has a recursive relation similar to (3) and consequently, can be expressed by using an objective function $A_K(z)$ for the extension of $Q_{K-1}(z)_{LHBP}$ to $Q_K(z)$ as below

$$Q_K(z) = Q_{K-1}(z)_{LHBP} + A_K(z) \tag{A.2}$$

where $Q_{K-1}(z)_{LHBP}$ is a LHBP filter of order $4K-6$, which is obtained from (3) as

$$\begin{aligned} Q_{K-1}(z)_{LHBP} = & z^{K-1}\left(\frac{1+z^{-1}}{2}\right)^{2(K-1)} \\ & \times \sum\nolimits_{\ell=0}^{K-2} d_{K-1,\ell}\left(\frac{2-z-z^{-1}}{4}\right)^{\ell} \end{aligned} \tag{A.3}$$

and the objective function $A_K(z)$ is defined by using two unknown coefficients c_{K-1} and c_K as

$$\begin{aligned} A_K(z) = & z^{K-1}\left(\frac{1+z^{-1}}{2}\right)^{2(K-1)} \\ & \times \left\{ c_{K-1}\left(\frac{(2-z-z^{-1})}{4}\right)^{K-1} \right. \\ & \left. + c_K\left(\frac{(2-z-z^{-1})}{4}\right)^{K} \right\} \end{aligned} \tag{A.4}$$

From (A.2) $Q_K(z)$ can be rewritten as

$$Q_K(z) = z^{K-1}\left(\frac{1+z^{-1}}{2}\right)^{2(K-1)}$$

$$\times \left\{ \sum_{\ell=0}^{K-2} d_{K-1,\ell} \left(\frac{2-z-z^{-1}}{4} \right)^{\ell} + c_{K-1} \left(\frac{(2-z-z^{-1})}{4} \right)^{K-1}, + c_K \left(\frac{(2-z-z^{-1})}{4} \right)^{K} \right\} \tag{A.5}$$

For mapping this polynomial into a general form of (11), using the transformation

$$\left(\frac{2-z^{-1}-z}{4} \right)^{\ell} \Bigg|_{z=e^{j\omega}} = \frac{1}{2^{2\ell}} \left\{ \binom{2\ell}{\ell} + 2\sum_{j=1}^{\ell} (-1)^j \binom{2\ell}{\ell-j} \frac{z^j+z^{-j}}{2} \Bigg|_{z=e^{j\omega}} \right\} \tag{A.6}$$

on (A.5) and simplifying in a similar way of [10], we can obtain g_ℓ's which are expressed in terms of c_{K-1} and c_K as

$$g_\ell = (-1)^{K-\ell} \sum_{j=2}^{\ell} \frac{d_{K-1,K-j}}{2^{2(K-j)}} \binom{2(K-j)}{\ell-j} + (-1)^{K-\ell} \left\{ \frac{c_{K-1}}{2^{2(K-1)}} \binom{2(K-1)}{\ell-1} + \frac{c_K}{2^{2K}} \binom{2K}{\ell} \right\} \tag{A.7}$$

where $\binom{A}{B} = 0$, if $A < B$ or $B < 0$.

From (A.7) and (13) g_0, g_1, h_0, and h_1 are given respectively as

$$g_0 = (-1)^K \frac{c_K}{2^{2K}} \text{ and } g_1 = (-1)^{K-1} \times \left\{ \frac{c_{K-1}}{2^{2(K-1)}} + \frac{c_K}{2^{2K}} \binom{2K}{1} \right\} \tag{A.8}$$

$$h_0 = \frac{g_0}{2^{2(K-1)}} \text{ and } h_1 = \frac{1}{2^{2(K-1)}} \times \left\{ \binom{2(K-1)}{1} g_0 + g_1 \right\} = 0 \tag{A.9}$$

where $h_1 = 0$ results from h_{2n-1}'s $= 0$ given in (A.1). Substituting (A.8) into (A.9) yields c_{K-1} and c_K which are expressed in terms of h_0 as

$$c_{K-1} = (-1)^{K-1} 2^{4K-3} h_0 \tag{A.10}$$

$$c_K = (-1)^K 2^{4K-2} h_0 \tag{A.11}$$

By substituting these results into (A.4), (A.5), and (A.7), we can have respectively

$$A_K(z) = (-1)^{K-1} 2^{4K-2} h_0 z^{K-1} \left(\frac{(1+z^{-1})}{2} \right)^{2(K-1)} \times \left\{ \frac{1}{2} \left(\frac{(2-z-z^{-1})}{4} \right)^{K-1} - \left(\frac{(2-z-z^{-1})}{4} \right)^{K} \right\} \tag{A.12}$$

$$Q_K(z) = z^{K-1} \left(\frac{1+z^{-1}}{2} \right)^{2(K-1)} \left\{ \sum_{\ell=0}^{K-2} d_{K-1,\ell} \times \left(\frac{2-z-z^{-1}}{4} \right)^{\ell} + (-1)^{K-1} 2^{4K-2} h_0 \times \left[\frac{1}{2} \left(\frac{2-z-z^{-1}}{4} \right)^{K-1} - \left(\frac{2-z-z^{-1}}{4} \right)^{K} \right] \right\} \tag{A.13}$$

$$\begin{aligned} g_\ell &= (-1)^{K-\ell} \sum_{j=2}^{\ell} \frac{d_{K-1,K-j}}{2^{2(K-j)}} \binom{2(K-j)}{\ell-j} + (-1)^{2K-1-\ell} 2^{2K-1} h_0 \left\{ \binom{2(K-1)}{\ell-1} - \frac{1}{2} \binom{2K}{\ell} \right\} \\ &= (-1)^{K-\ell} \sum_{j=2}^{\ell} \frac{d_{K-1,K-j}}{2^{2(K-j)}} \binom{2(K-j)}{\ell-j} + (-1)^{\ell+1} 2^{2K-1} h_0 \left\{ \binom{2(K-1)}{\ell-1} - \frac{1}{2} \binom{2K}{\ell} \right\} \end{aligned} \tag{A.14}$$

REFERENCES

[1] J. F. Kaiser, "Design subroutine (MAXFLAT) for symmetric FIR lowpass digital filters with maximally-flat pass and stop bands," in *Program for Digital Signal Processing*. New York, NY, USA: IEEE Press, 1979, ch. 5, Sec. 3, pp. 1–6.

[2] P. Vaidyanathan, "Efficient and multiplierless design of FIR filters with very sharp cutoff via maximally flat building blocks," *IEEE Trans. Circuits Syst.*, vol. CS-32, no. 3, pp. 236–244, Mar. 1985.

[3] P. Vaidyanathan, "Optimal design of linear phase FIR digital filters with very flat passbands and equiripple stopbands," *IEEE Trans. Circuits Syst.*, vol. CS-32, no. 9, pp. 904–917, Sep. 1985.

[4] C.-C. Tseng and S.-L. Lee, "Design of linear phase FIR filters using fractional derivative constraints," *Signal Process.*, vol. 92, no. 5, pp. 1317–1327, May 2012.

[5] M. D. Kusljevic, J. J. Tomic, and P. D. Poljak, "Maximally flat-frequency-response multiple-resonator-based harmonic analysis," *IEEE Trans. Instrum. Meas.*, vol. 66, no. 12, pp. 3387–3398, Dec. 2017.

[6] T. Yoshida and N. Aikawa, "Low-delay band-pass maximally flat FIR digital differentiators," *Circuits, Syst., Signal Process.*, vol. 37, no. 8, pp. 3576–3588, Aug. 2018.

[7] O. Herrmann, "On the approximation problem in nonrecursive digital filter design," *IEEE Trans. Circuit Theory*, vol. CT-18, no. 3, pp. 411–413, May 1971.

[8] J. A. Miller, "Maximally flat nonrecursive digital filters," *Electron. Lett.*, vol. 8, no. 6, pp. 157–158, Mar. 1972.

[9] L. Rajagpoal and S. D. Roy, "Design of maximally-flat FIR filters using the bernstein polynomial," *IEEE Trans. Circuits Syst.*, vol. CS-34, no. 12, pp. 1587–1590, Dec. 1987.

[10] M. U. A. Bromba and H. Ziegler, "Explicit formula for filter function of maximally flat nonrecursive digital filters," *Electron. Lett.*, vol. 16, no. 24, pp. 905–906, Nov. 1980.

[11] P. Thajchayapong, M. Puangpool, and S. Banjongjit, "Maximally flat FIR filter with prescribed cutoff frequency," *Electron. Lett.*, vol. 16, no. 23, pp. 514–515, Jun. 1980.

[12] B. C. Jinaga and S. C. D. Roy, "Coefficients of maximally flat low and high pass nonrecursive digital filters with specified cutoff frequency," *Signal Process.*, vol. 9, no. 2, pp. 121–124, Sep. 1985.

[13] J. Jeon and D. Kim, "Design of nonrecursive FIR filters with simultaneously MAXFLAT magnitude and prescribed cutoff frequency," *Digit. Signal Process.*, vol. 22, no. 6, pp. 1085–1094, Dec. 2012.

[14] C.-C. Tseng and S.-L. Lee, "Closed-form designs of digital fractional order butterworth filters using discrete transforms," *Signal Process.*, vol. 137, pp. 80–97, Aug. 2017.

[15] X. Huang, B. Zhang, H. Qin, and W. An, "Closed-form design of variable fractional-delay FIR filters with low or middle cutoff frequencies," *IEEE Trans. Circuits Syst. I, Reg. Papers*, vol. 65, no. 2, pp. 628–637, Feb. 2018.

[16] R. Ma, Y. Wang, W. Hu, X. Zhu, and K. Zhang, "Optimum design of multistage half-band FIR filter for audio conversion using a simulated annealing algorithm," in *Proc. 13th IEEE Conf. Ind. Electron. Appl. (ICIEA)*, May 2018, pp. 74–78.

[17] N. Haridas and E. Elias, "Reconfigurable farrow structure-based FRM filters for wireless communication systems," *Circuits, Syst., Signal Process.*, vol. 36, no. 1, pp. 315–338, Jan. 2017.

[18] L. M. San-José-Revuelta and J. I. Arribas, "A new approach for the design of digital frequency selective FIR filters using an FPA-based algorithm," *Expert Syst. Appl.*, vol. 106, pp. 92–106, Sep. 2018.

[19] T. S. Bindiya and E. Elias, "Design of totally multiplier-less sharp transition width tree structured filter banks for non-uniform discrete multitone system," *AEU-Int. J. Electron. Commun.*, vol. 69, no. 3, pp. 655–665, Mar. 2015.

[20] S.-C. Pei and P.-H. Wang, "Closed-form design and efficient implementation of generalized maximally flat half-band FIR filters," *IEEE Signal Process. Lett.*, vol. 7, no. 6, pp. 149–151, Jun. 2000.

[21] M. M. J. Yekta, "Equivalence of the Lagrange interpolator for uniformly sampled signals and the scaled binomially windowed shifted sinc function," *Digit. Signal Process.*, vol. 19, no. 5, pp. 838–842, Sep. 2009.

[22] R. Ansari, C. Guillemot, and J. F. Kaiser, "Wavelet construction using Lagrange halfband filters," *IEEE Trans. Circuits Syst.*, vol. 38, no. 9, pp. 1116–1118, Sep. 1991.

[23] G. Anbarjafari and H. Demirel, "Image super resolution based on interpolation of wavelet domain high frequency subbands and the spatial domain input image," *ETRI J.*, vol. 32, no. 3, pp. 390–394, Jun. 2010.

[24] B.-R. Horng and A. N. Willson, "Lagrange multiplier approaches to the design of two-channel perfect-reconstruction linear-phase FIR filter banks," *IEEE Trans. Signal Process.*, vol. 40, no. 2, pp. 364–374, Feb. 1992.

[25] J. Rodrigues and K. R. Pai, "New approach to the synthesis of sharp transition FIR digital filter," in *Proc. IEEE Int. Symp. Ind. Electron. (ISIE)*, vol. 3, Jun. 2005, pp. 1171–1173.

[26] X. Huang, S. Jing, Z. Wang, Y. Xu, and Y. Zheng, "Closed-form FIR filter design based on convolution window spectrum interpolation," *IEEE Trans. Signal Process.*, vol. 64, no. 5, pp. 1173–1186, Oct. 2015.

[27] X. Huang, Y. Wang, Z. Yan, H. Xian, and M. Liu, "Closed-form FIR filter design with accurately controllable cut-off frequency," *Circuits, Syst., Signal Process.*, vol. 36, no. 2, pp. 721–741, Feb. 2017.

[28] S. Roy and A. Chandra, "Design of narrow transition band digital filter: An analytical approach," *Integration*, vol. 68, pp. 38–49, Sep. 2019.

[29] S. Roy and A. Chandra, "A survey of FIR filter design techniques: Low-complexity, narrow transition-band and variable bandwidth," *Integration*, vol. 77, pp. 193–204, Mar. 2021.

[30] I. R. Khan and R. Ohba, "Efficient design of halfband low/high pass FIR filters using explicit formulas for tap-coefficients," *IEICE Trans. Fundament.*, vol. 83, no. 11, pp. 2370–2373, Nov. 2000.

[31] I. R. Khan, "Flat magnitude response FIR halfband low/high pass digital filters with narrow transition bands," *Digital Signal Process.*, vol. 20, no. 2, pp. 328–336, Mar. 2010.

WOON CHO received the bachelor's degree from the Department of Information and Communication Engineering, Dongguk University, Seoul, South Korea, in 2014, where he is currently pursuing the combined master's and Ph.D. degrees in electronics and electrical engineering. Since 2016, he has been lecturing in computers and networks. His current research interests include digital design filter, medical image processing, edge detection, and deep learning.

DAEWON CHUNG received the bachelor's degree from the Department of Information and Communication Engineering, Dongguk University, Seoul, South Korea, in 2015, where he is currently pursuing the integrated master's and Ph.D. degrees in electronics and electrical engineering.

Since 2016, he has been lecturing in computers application and visual programming. His current research interests include digital filter design, signal and image processing, such as enhancement and restoration, edge detection, and deep learning with computer vision.

YUNSUN KIM received the bachelor's degree from the Department of Electronics Engineering, Chosun University, in 2019. He is currently pursuing the combined master's and Ph.D. degrees in electronics and electrical engineering with Dongguk University, Seoul, South Korea. His current research interests include computer vision, super resolution, digital image processing based on AI, and deep learning.

INGYUN KIM received the bachelor's degree from the Department of Electronics and Electrical Engineering, Dongguk University, Seoul, South Korea, in 2020, where he is currently pursuing the master's degree with the Division of Electronics and Electrical Engineering. His current research interests include time series forecasting, object detection, digital image processing based on AI, and deep learning.

JOONHYEON JEON received the B.S. degree in electronic engineering from Dongguk University, Seoul, South Korea, in 1984, and the M.S. and Ph.D. degrees in electric and electronic engineering from the Korea Advanced Institute of Science and Technology, South Korea, in 1986 and 1991, respectively. From 1991 to 1999, he was a Project Manager with the Korea Telecom Research Center, Department of Image Processing, where he was responsible for the development of network-oriented video service systems. He is currently an Associate Professor with the Department of Electronics and Electrical Engineering, Dongguk University. His current research interests include digital image processing and transmission, theory and application of wavelet transforms, and digital filter design.